

Air trapping in Wegener's granulomatosis: an additional finding on expiratory chest HRCT

L'intrappolamento d'aria nella granulomatosi di Wegener: un reperto integrativo nella HRCT eseguita in espirazione

E. Magkanas¹ • E. Detorakis¹ • I. Nikolakopoulos¹ • S. Gourtsoyianni¹ • M. Linardakis³
P. Sidiropoulos² • D. Boumpas² • N. Gourtsoyiannis¹

¹Department of Radiology, University Hospital of Heraklion, Medical School of Crete, 71110 Stavrakia, Heraklion, Crete, Greece

²Department of Rheumatology, University Hospital of Heraklion, Medical School of Crete, Heraklion, Crete, Greece

³Department of Preschool Education, University of Crete, Greece

Correspondence to: E. Magkanas, 1 Tsakiri St., 71202, Heraklion, Crete, Greece, Tel.: +30-2810-392542, Fax: +30-2810-542095, e-mail: emagkanas@gmail.com; E. Detorakis, Tel.: +30-6973-037859, e-mail: edetorakis@hotmail.com

Received: 31 August 2010 / Accepted: 24 November 2010 / Published online: 21 April 2011

© Springer-Verlag 2011

Abstract

Purpose. This study was undertaken to assess the presence and extent of air trapping (AT) on high-resolution computed tomography (HRCT) in patients with Wegener's granulomatosis (WG) and to correlate the finding with the inspiratory pattern and bronchial/bronchiolar involvement. **Materials and methods.** Twenty-one patients (7 M/14 F) with WG underwent inspiratory and expiratory HRCT. Images were evaluated for the presence and extent of AT and for airway involvement (bronchi/bronchioles); the predominant HRCT pattern was also documented. The attenuation difference was measured between the areas of AT on expiration and the same areas on inspiration in order to verify the finding of AT. The extent of AT was calculated by visual scoring and correlated with the predominant inspiratory patterns and bronchial/bronchiolar involvement. **Results.** AT was found in seven patients (33.3%) and its extent ranged between 3% and 70% (mean 15.8±7). Two patients showed no lesions on inspiratory HRCT, and the only finding was AT on expiration. The attenuation difference between areas of AT on expiration and the same areas on inspiration ranged between 32 and 89 HU. Inspiratory HRCT was pathological in 19 patients (90.4%), and the principal lung patterns were nodular, cavitory or noncavitory (n=7, 38.9%); ground-glass opacities (n=5, 26.3%); masses (n=3, 15.8%); fibrotic (n=3, 15.8%); and consolidation with air bronchogram (n=1, 5.3%). Bronchial and bronchiolar involvement was found in 14 and five patients, respectively. No statistically significant

Riassunto

Obiettivo. Scopo di questo studio è quello di valutare la presenza e l'estensione dell'intrappolamento d'aria nella granulomatosi di Wegener (GW) attraverso l'utilizzo della tomografia computerizzata ad alta risoluzione (HRCT) e correlare con i reperti inspiratori ed il coinvolgimento bronchiale/bronchiolare. **Materiali e metodi.** 21 pazienti (7M/14F) affetti da WG sono stati esaminati con HRCT in fase inspiratoria ed espiratoria. Le immagini sono state valutate per la presenza e l'estensione di intrappolamento d'aria, per il coinvolgimento delle vie aeree (bronchi/bronchioli) ed il modello HRCT dominante. È stata misurata la differenza di attenuazione tra le regioni di intrappolamento d'aria e le corrispondenti regioni in inspirazione per poter verificare la presenza di intrappolamento d'aria. L'estensione di intrappolamento d'aria è stata calcolata con calcolo visuale (visual scoring) e correlata con il modello inspiratorio dominante e il coinvolgimento bronchiale/bronchiolare. **Risultati.** L'intrappolamento d'aria è stato identificato in 7 (33,3%) e la sua estensione era tra il 3% ed il 70% (15,8±7). Due dei pazienti non avevano presentato dei reperti in fase inspiratoria ed il loro unico reperto era l'intrappolamento d'aria in fase espiratoria. La differenza di attenuazione tra le regioni d'intrappolamento d'aria in espirazione e le stesse regioni in inspirazione aveva un range compreso tra 32 e 89 unità di Hounsfield (HU). La TC ad alta

correlation was found between AT extent and the findings on inspiration. In addition, there were no specific patterns that caused higher or lower scores of AT. Moreover, when bronchial or bronchiolar involvement was absent, the mean AT score was statistically significantly higher.

Conclusions. Areas of AT represent a new and indirect HRCT finding, – and in rare cases the only finding – of pulmonary WG. The nonsignificant correlation between AT extent and inspiratory findings may suggest AT as an additional HRCT finding in patients with WG.

Keywords Wegener's granulomatosis · Bronchiolectasis · Air trapping

risoluzione era patologica in 19 pazienti (90,4%) e rappresentata dai seguenti modelli polmonari principali: nodulare, cavitario/non cavitario (n=7, 38,9%), opacità a vetro smerigliato (GGO) (n=5, 26,3%), masse (n=3, 15,8%), modello fibrotico (n=3, 15,8%) e consolidativo con broncogramma aereo (n=1, 5,3%). Il coinvolgimento dei bronchi e bronchioli è stato riscontrato in 14 e 5 pazienti rispettivamente. Non è stata rilevata una correlazione statisticamente significativa tra l'estensione dell'intrappolamento d'aria ed i reperti in fase inspiratoria. Inoltre, non ci sono dei modelli specifici che possono causare dei livelli alti o bassi d'intrappolamento d'aria. Per di più, quando il coinvolgimento bronchiale o bronchiolare è assente il valore medio dei livelli d'intrappolamento d'aria è statisticamente e significativamente più elevato.

Conclusioni. *Le regioni d'intrappolamento d'aria nella granulomatosi di Wegener, rappresentano un nuovo reperto, indiretto e probabilmente, in rari casi, l'unico reperto di coinvolgimento polmonare rilevato in TC ad alta risoluzione. La correlazione non statisticamente significativa tra l'estensione dell'intrappolamento d'aria ed i reperti in fase inspiratoria possono suggerire l'intrappolamento d'aria come un ulteriore reperto nella TC ad alta risoluzione in pazienti con granulomatosi di Wegener.*

Parole chiave Granulomatosi di Wegener · Bronchiolettasia · Intrappolamento d'aria

Introduction

First described by Friedrich Wegener in the late 1930's, Wegener's granulomatosis (WG) is a rare systemic autoimmune disorder characterised histologically by a necrotising granulomatous vasculitis that most commonly involves the lungs, nasal pathways, paranasal sinuses and kidneys, but may affect any organ system [1–3]. The disease traditionally belongs to the group of diffuse interstitial lung diseases that, according to a recent classification, has been renamed diffuse parenchymal lung diseases [4]. It follows a chronic relapsing course, and the respiratory tract is the most commonly involved system. Upper respiratory tract disease is reported in up to 90% and lung involvement in 70–90% of patients [5]. The disease involves the subglottic part of the airways, mainly the trachea and the main bronchi, causing bronchial wall thickening and airway lumen stenosis [1, 2]. To our knowledge, little is known about small airway involvement by the disease, especially as regards subsegmental bronchi and bronchioles.

The primary aim of this study was to document the inspiratory high-resolution computed tomography (HRCT)

patterns and airway involvement as well as expiratory findings in patients with known WG. Disease assessment consisted of documenting the presence and extent of air trapping (AT) on expiratory HRCT scans and correlating it with the inspiratory HRCT patterns and with the extent of bronchial and bronchiolar involvement, as studied on deep inspiratory and deep expiratory chest HRCT images.

Materials and methods

Patients

Between April 1999 and January 2009, 23 consecutive patients, 14 women and 9 men with an age range between 18 and 72 (mean 45) years were retrospectively studied. Twenty-one of these patients were newly diagnosed with WG, whereas two had been diagnosed 7 and 8 years, respectively, before the HRCT scans were performed. Two of these patients were active smokers (mean 20 pack-years) and

were excluded from the study, whereas among the remaining 21 patients, two were former smokers having ceased smoking 7 and 10 years, respectively, before the study began. None of the 21 patients had previous lung disease, including asthma, chronic obstructive pulmonary disease, pulmonary embolism or primary pulmonary hypertension. All were inpatients of our hospital's rheumatology department with acute-phase disease. Initial pulmonary evaluation involved history taking, auscultation and chest radiography (frontal and lateral views). Seven patients had signs and symptoms of active lower respiratory tract disease consisting of nonproductive cough, mild dyspnoea and haemoptysis. At the time of examination, all 21 patients presented with a positive serum titre for anticytoplasmic antibodies (cANCA), whereas 12 of them were positive for anti-PR3 antibodies.

The clinical diagnosis of WG was established in accordance with the 1990 American College of Rheumatology Criteria [6] and the Chapel Hill criteria [7]. Diagnosis was histologically confirmed by biopsy in all patients. Trans-bronchial biopsy was performed in four patients, video-assisted thoracoscopy (VAT) in two, open lung biopsy in one, renal biopsy in seven, nasal mucosa biopsy in four and skin and subcutaneous tissue biopsy in three. All patients underwent paired inspiratory and expiratory chest HRCT scan.

HRCT

The examinations consisted of obtaining paired end-inspiratory and end-expiratory thin-section HRCT scans in the supine position. Before each examination, patients were instructed to take a deep breath before the inspiratory scan and to deeply exhale before the expiratory scan. Pulmonary HRCT was performed either with a conventional CT scanner (Philips Tomoscan LX scanner, Philips Medical Systems, Best, The Netherlands) (reconstruction matrix 512×512, 130 kVp, 174 mAs tube current, scan time 1.9 s, slice thickness 1.5 mm, 10-mm spacing on inspiration and 20-mm on expiration) or with a 16-slice CT scanner (Siemens Somatom Sensation 16, Erlangen, Germany) (120 kVp, 100 mAs tube current, scan time 0.75 s, slice collimation 0.75 mm and pitch factor 1.5). In each patient, sequential inspiratory scanning sequences were acquired at 10-mm intervals from the level of the lung apices to below the costophrenic angles, and expiratory HRCT scans were acquired with a 20-mm interval. All images were reconstructed using a high-spatial frequency reconstruction algorithm.

Two experienced chest radiologists independently examined the HRCT images in random order and recorded the presence and extent of findings by visual assessment. Expiratory scans were studied first in order to avoid any bias in the interpretation of areas of AT documented on expira-

tion from the identification of inspiratory findings, such as nodules and airway involvement. In cases of discordant interpretations, the images were re-evaluated together with a third chest radiologist. A final decision was then reached in consensus between the three radiologists.

On inspiration, the scans were visualised at two different window settings: one appropriate for lung parenchyma (width 1,400/level; 700 HU) and one (width 1,000/level; 600 HU) for scoring slight attenuation differences in the lung parenchyma.

The predominant parenchymal pattern – nodules and masses (cavitated or not), ground-glass opacities, consolidation areas and honeycombing as a sign of lung fibrosis – was evaluated on inspiratory HRCT scan. On inspiratory scans, airway involvement was evaluated on the basis of wall thickening of the trachea and bronchi, bronchiectasis and bronchiolectasis. The presence or absence of bronchial and bronchiolar wall thickening was assessed considering that the wall thickness of conducting bronchi and bronchioles of <5 mm in calibre should normally measure one sixth to one tenth of their diameter [8]. Hence, in every patient with suspected airway wall thickening, we calculated the ratio between the bronchial wall thickness (T) and total diameter of the bronchus (D), which in normal individuals is 0.2, or 20%, on average [9].

To assess possible airway dilation, a comparison was made between the internal diameter of the bronchus and the diameter of the adjacent pulmonary artery branch measured at sea level [10]. To this end, we calculated the bronchoarterial ratio, defined as the ratio between the bronchial luminal diameter (L) and the diameter (d) of its accompanying artery. Both L and d and the previously described T and D were magnified 1.5–1.8 times and measured using electronic callipers. A bronchoarterial ratio >1 was considered typical of bronchiectasis, as was visualisation of a bronchus within <2 cm of the costal pleura or abutting the mediastinal pleura. Multiplanar reformation images displayed in minimum intensity projection (min-IP) were extremely helpful in demonstrating the presence or absence of tracheobronchial stenosis.

On expiration, the presence of AT was scored and its extent calculated by visual assessment. According to the Nomenclature Committee of the Fleischner Society, AT is a pathophysiological term that indicates the retention of excess air in all or part of the lung at any stage of expiration [11]. To assess the presence or absence of AT, small regions of interest (ROIs) 1–2 cm in diameter including at least 95 pixels each were drawn freehand to measure the attenuation difference in Hounsfield units between areas of low attenuation on expiration and corresponding areas on inspiration. To obtain a more accurate assessment of AT, ROIs did not include vessels or regions close to lung fissures or the chest wall.

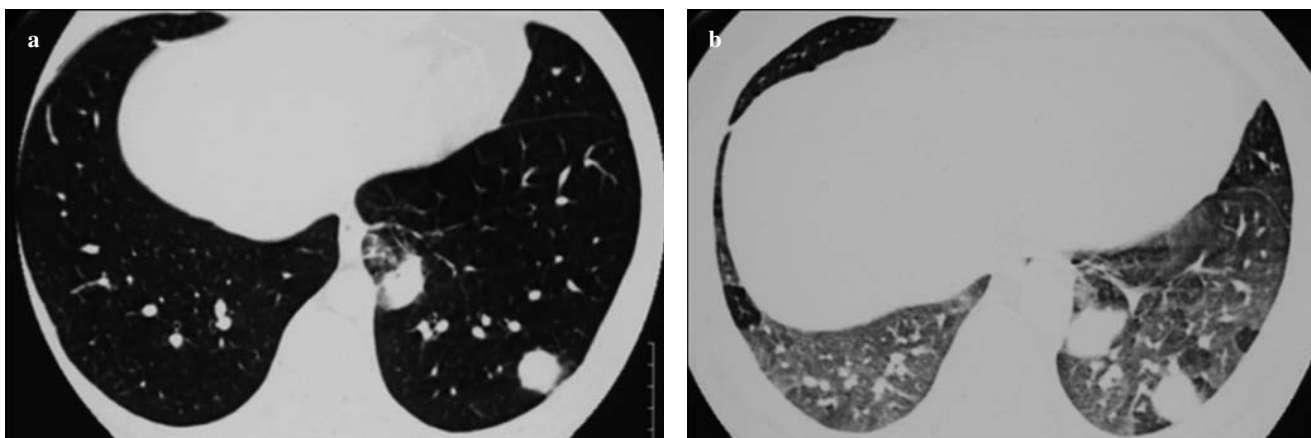


Fig. 1a Inspiratory chest high-resolution computed tomography (HRCT) scan. In the left lower lobe, a large nodule with peripheral ground-glass opacity can be seen. **b** Expiratory HRCT at the same level shows geographically distributed areas of air trapping in both lung bases.

Fig. 1a HRCT torace eseguita in inspirazione: al livello del lobo inferiore sinistro si evidenzia un grande nodulo circoscritto da una zona a vetro smerigliato. **b** HRCT eseguita in espirazione allo stesso livello presenta delle zone d'intrappolamento d'aria distribuita a carta geografica in ambedue le basi polmonari.

AT extent was classified as lobular when composed of hypoattenuation areas corresponding to fewer than three adjacent secondary pulmonary lobules in one or two regions per lung level, as segmental when corresponding to a pulmonary segment or three or more adjacent secondary pulmonary lobules, and as lobar when the hypoattenuation area was more extended than a pulmonary segment. In patients showing multiple AT patterns, the most extensive one (lobar rather than segmental; segmental rather than lobular) was taken in consideration [12, 13].

Subsequently, the extent of AT areas was evaluated by visual assessment using a semiquantitative scoring system estimating the percentage of lung that appeared abnormal on each scan [14]. To this end, two experienced chest radiologists were recruited who were blinded to patients' clinical information and disease severity. A 5-point scoring system, similar to the one proposed by Webb et al. [14, 15] and Stern et al. [16], was used to estimate AT on expiratory scans in three different lung fields for each lung to a total of six lung fields for both lungs: upper lung fields, from the lung apices to just above the level of the carina; middle lung fields between the level of the carina and the pulmonary veins; inferior lung fields from the pulmonary vein level to the level of the diaphragm. At each level and for each lung, a 5-point scale was used to estimate the percentage of AT extent visible to each radiologist: 0 for no AT; 1 for AT between 1% and 25% of the cross-sectional area of the affected lung; 2 for AT between 26% and 50%; 3 for AT from 51% to 75%; 4 for AT between 76% and 100% [14–16]. In the event of discordance between the two radiologists, images were re-evaluated together with a third chest radiologist, and a final consensus opinion was reached.

Statistical analysis

Due to the small sample size, data were analysed using non-parametric statistical tests. More specifically, the Mann–Whitney and Kruskal–Wallis tests were used to examine statistically significant differences between two mean values or among three or more mean values, respectively. Furthermore, Spearman's rho nonparametric correlation coefficient was used to investigate pairwise relationships between continuous variables. All analyses were performed using the statistical package SPSS-PASW version 18. The aim of the analyses was to correlate the extent of AT on expiration with the predominant inspiratory HRCT pattern and its total extent on inspiration as well as with airway involvement.

Results

On expiratory chest HRCT, AT areas were observed in seven (33.3%) of 21 patients, and the percentage of disease extent ranged between 3% and 70.8% (mean value 15.8 ± 7) (Fig. 1). Three patterns of AT distribution were documented: lobular in two patients (9.5%), segmental in four (19%) and lobar in one (4.7%). In six (28.5%) of seven patients, AT was found to be multifocal (Fig. 1).

According to the 5-point scale used for AT extent, two patients (9.5%) scored 0, 16 (84.2%) scored 1, three (14.3%) scored 2 and none scored 3 or 4. AT areas were observed in all six lung fields (three for each lung) and were distributed: bilaterally in the lower lung fields in all seven patients (100%), in the upper lung fields in four (51.7%) and in the middle lung fields in three (42.9%); in two, the

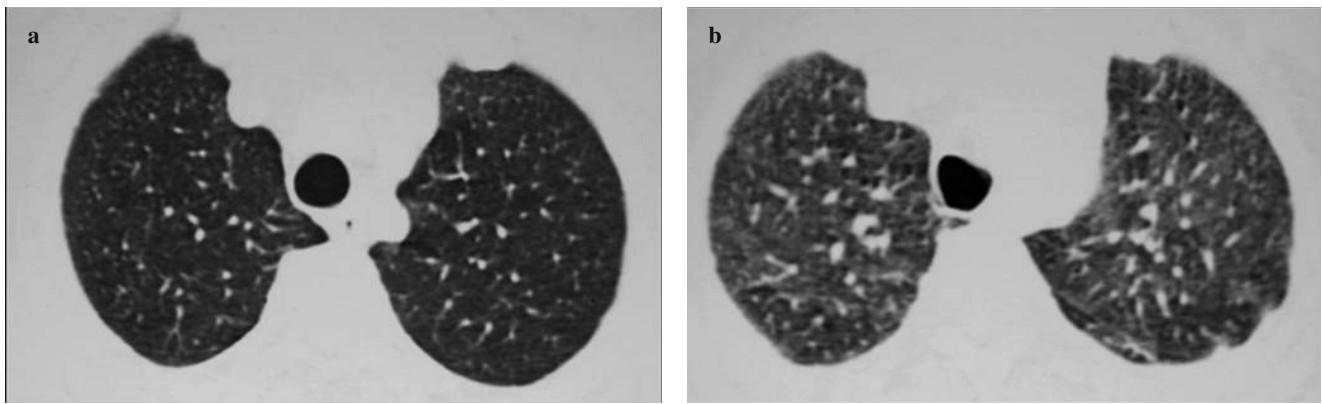


Fig. 2a,b A 29-year-old nonsmoker, with no known previous lower respiratory tract disease. **a** On inspiratory high-resolution computed tomography (HRCT), no abnormal findings are seen in the upper lung fields; **b** on deep expiratory HRCT, areas of air trapping are demonstrated in a patchy and segmental distribution bilaterally.

Fig. 2a,b Paziente di 29 anni, non fumatore, senza patologia nota delle vie respiratorie inferiori. **a** In HRCT eseguita in inspirazione, non si registrano reperti patologici nelle aree polmonari superiori; **b** in HRCT eseguita in espirazione profonda, zone d'intrappolamento d'aria si visualizzano bilateralmente a distribuzione segmentaria "a macchie".

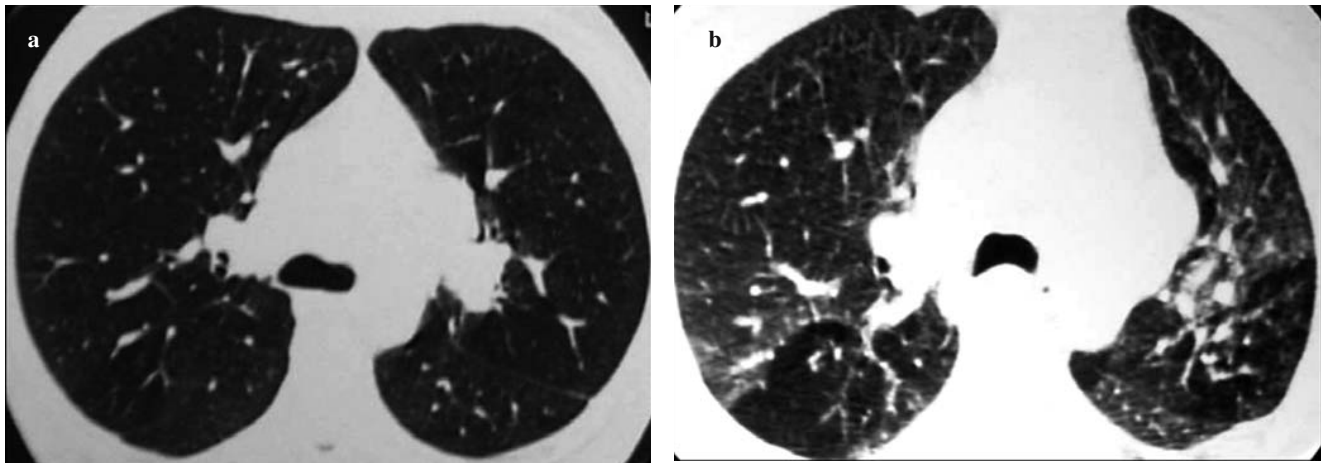


Fig. 3a On inspiratory high-resolution computed tomography (HRCT) at the level of the carina, only some small nodules can be seen in a peribronchovascular distribution; **b** areas of air trapping are depicted on expiratory HRCT in both lungs in a segmental distribution.

Fig. 3a In HRCT eseguita in inspirazione a livello della carena tracheale si identificano soltanto alcuni piccoli noduli a distribuzione peribroncovascolare. **b** Zone d'intrappolamento d'aria a distribuzione segmentaria si evidenziano in entrambi i polmoni in HRCT eseguita in espirazione.

AT areas were unilateral in the upper lung fields. Among these seven patients, two nonsmokers showed AT areas on expiratory and no HRCT findings on inspiratory scans (Fig. 2). It is important to emphasise that a good interobserver agreement was achieved in AT evaluation. In these seven (33.3%) patients, the attenuation difference of the AT areas ranged between -627 HU and -807 HU (mean -725.2 ± 44.6 HU) on expiration and between -705 HU and -856 HU (mean -789 ± 51.4 HU) on inspiration (Fig. 3). The expected mean attenuation difference in normal lungs between full inspiration and expiration usually ranges from 80 to 300 HU. On dynamic scans, a lung attenuation difference <70

or 80 HU between full inspiration and full exhalation may be regarded as abnormal [14]. In our study group, the attenuation difference between inspiration and expiration ranged from 32 to 89 HU (mean 60 ± 23.5 HU), whereas the attenuation measurements in the adjacent normal parenchyma ranged between -710 HU and -885 HU (mean -795.4 ± 61.7 HU) on inspiratory scans and from -640 HU to -775 HU (mean -695 ± 58.9 HU) on expiratory scans, with a difference between inspiration and expiration that ranged from 100 HU to 250 HU.

Nineteen of 21 patients presented with HRCT findings on inspiratory scans. The predominant patterns were nodu-



Fig. 4 Inspiratory chest high-resolution computed tomography (HRCT) scan at the level of the right main bronchus shows thickening of the bronchial wall of the right upper lobar bronchus and its posterior and apical branches. Two cavitated nodules can be distinguished in close contact with the wall of the latter.

Fig. 4 HRCT del torace in inspirio al livello del bronco principale di destra evidenzia ispessimento della parete bronchiale del bronco lobare superiore di destra e dei suoi rami posteriori e apicali. Sono riconoscibili due noduli con cavità all'interno in contatto con le pareti bronchiali.

lar (cavitated or not) in seven patients (38.9%) (Figs. 1a, 3a, 4), ground-glass opacities in five (26.3%) (Figs. 5, 6), masses (cavitated or not) in three (15.8%) (Fig. 5), honeycombing revealing a fibrotic pattern in three (15.8%) and consolidation areas with air bronchogram in one (5.3%). Two patients did not present any abnormal HRCT findings

on inspiration (Table 1). Fourteen of the 21 patients had airway involvement: nine (42.8%) showed bronchiectasis and five (23.8%) bronchial wall thickening. In addition, five patients (23.8%) had bronchiolectasis and two (9.5%) had bronchiolar wall thickening (Fig. 6). [CE1]. It is important to mention that none of the patients exhibited wall thickening of the trachea or the main bronchi, as commonly mentioned in literature [1–3, 9].

The extent of the inspiratory and expiratory findings was expressed in percentage of lung involvement related to the remaining normal parenchyma, and this ranged between 0% and 36.7% (mean value 10.5 ± 11.4). Spearman's correlation coefficient between inspiration and expiration was $r = -0.125$, which is not statistically significant ($p > 0.1$). This means that if there are no inspiratory findings in a patient, this does not indicate absence of expiratory findings. The opposite may also happen: a patient with expiratory findings may have no indication of the disease on inspiration. Hence, it is strongly suggested that both inspiration and expiration should be examined simultaneously. In addition, the Kruskal–Wallis test showed that specific inspiratory patterns such as bronchial and bronchiolar involvement do not influence the AT scores (all $p > 0.1$). Spearman's correlation coefficient between right and left lung AT scores was statistically highly significant ($r = 0.97$, $p < 0.01$), indicating that AT was diffusely distributed. In contrast, there was a weak positive correlation between the right and left lung scores on inspiration ($r = 0.385$, $p < 0.1$). Additionally, the Mann–Whitney test showed that when bronchial or bronchiolar involvement was absent, the mean AT score was statistically significantly higher ($p < 0.05$).

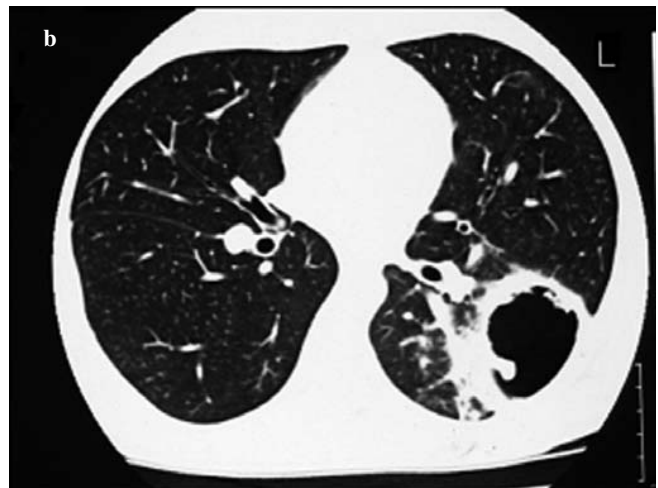


Fig. 5a,b Inspiratory chest high-resolution computed tomography (HRCT) scan. **a** In the mediastinal window a large cavitated mass with thick irregular walls is depicted, which seems to communicate with the peripheral airways. **b** In the lung window, the mass is surrounded by ground-glass opacity (CT halo sign, indicating pulmonary haemorrhage).

Fig. 5a,b HRCT del torace eseguita in inspirazione. a Nella finestra mediastinica viene visualizzata una grande massa cavitaria con pareti spesse e irregolari che appare comunicare con le vie aeree periferiche. b Nella finestra per parenchima polmonare la massa è circondata da opacità a vetro smerigliato (TC halo sign, che indica emorragia polmonare)

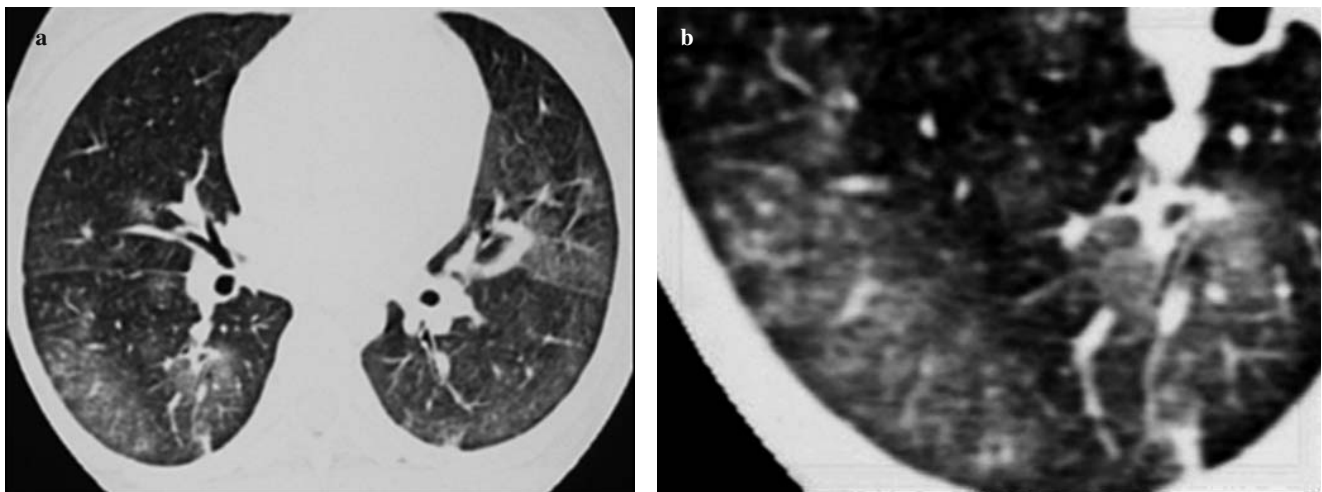


Fig. 6a Inspiratory chest high-resolution computed tomography (HRCT) scan at the level of the lower lung fields with ground-glass opacities dominating bilaterally; **b** magnified view in which we can distinguish areas with bronchiolectasis at the lung periphery.

Fig. 6a HRCT del torace eseguita in inspirazione con opacità a vetro smerigliato a livello dei lobi polmonari inferiori evidenziate bilateralmente; *b* Nell'immagine ingrandita possiamo distinguere delle bronchioloectasie periferiche.

Table 1 Percentage distribution of AT, inspiratory patterns and airway involvement

Patient	RU	LU	RM	LM	RL	LL	Total AT ^a	Predom. insp. pattern	Airway involvement ^b
1	0	0	0	0	0	0	0	Masses	B, BWT
2	0	0	0	0	0	0	0	Nodules	B
3	75	75	50	75	75	75	70.8	Normal	–
4	25	10	25	10	15	15	16.7	Ground glass	B
5	10	0	15	15	0	25	10.8	Honeycombing	–
6	10	15	0	15	0	15	9.2	Normal	B, bwt
7	0	0	0	0	0	0	0	Ground glass	B, BWT
8	0	0	0	0	0	0	0	Consolidation	B, BWT
9	0	0	0	0	0	0	0	Honeycombing	B
10	0	0	0	0	0	0	0	Masses	–
11	0	15	10	0	15	20	10	Nodules	–
12	0	0	0	0	0	0	0	Nodul	B, BWT
13	0	0	0	0	0	0	0	Nodules	B
14	0	0	0	0	0	0	0	Nodules	B
15	0	0	0	0	0	0	0	Masses	B
16	20	0	10	30	0	10	11.7	Ground glass	–
17	0	0	0	0	0	0	0	Nodules	B
18	35	20	30	0	0	20	17.5	Ground glass	–
19	0	0	0	0	0	0	0	Ground glass	B, BWT, br
20	0	0	0	0	0	0	0	Normal	–
21	0	0	0	0	0	0	0	Honeycombing	bwt, br
MV	8.33	5.71	7.38	6.90	16.60	8.57	6.98		
SD	18.19	4.77	13.28	17.42	5.00	17.40	15.83		

Lung fields: RU, right upper; LU, left upper; RM, right middle; LM, left middle; RL, right lower; LL, left lower

^aTotal air trapping: percentage of lung involvement by air trapping per patient

^bAirway involvement: B, bronchiectasis; BWT, bronchial wall thickening; br, bronchiolectasis; bwt, bronchiolar wall thickening

Tabella 1 Distribuzione percentuale di IA, lesioni inspiratorie e coinvolgimento delle vie aeree

Paziente	SD	SS	MD	MS	ID	IS	IA totale ^a	Pattern inspir. domin.	Coinvolgimento delle vie aeree ^b
1	0	0	0	0	0	0	0	Masse	B,IPB
2	0	0	0	0	0	0	0	Noduli	B
3	75	75	50	75	75	75	70.8	Normale	–
4	25	10	25	10	15	15	16.7	Vetro Smerigliato	B
5	10	0	15	15	0	25	10.8	Honeycombing	–
6	10	15	0	15	0	15	9.2	Normale	B, ipb
7	0	0	0	0	0	0	0	Vetro Smerigliato	B, IPB
8	0	0	0	0	0	0	0	Consolidazione	B, IPB
9	0	0	0	0	0	0	0	Honeycombing	B
10	0	0	0	0	0	0	0	Masse	–
11	0	15	10	0	15	20	10	Noduli	–
12	0	0	0	0	0	0	0	Noduli	B, IPB
13	0	0	0	0	0	0	0	Noduli	B
14	0	0	0	0	0	0	0	Noduli	B
15	0	0	0	0	0	0	0	Masse	B
16	20	0	10	30	0	10	11.7	Vetro Smerigliato	–
17	0	0	0	0	0	0	0	Noduli	B
18	35	20	30	0	0	20	17.5	Vetro Smerigliato	–
19	0	0	0	0	0	0	0	Vetro Smerigliato	B, IPB, br
20	0	0	0	0	0	0	0	Normale	–
21	0	0	0	0	0	0	0	Honeycombing	IPB, br
M.V	8.33	5.71	7.38	6.90	16.6	8.57	6.98		
S.d	18.19	4.77	13.28	17.42	5.00	17.40	15.83		

SD, superiore destro; SS, superiore sinistro; MD, medio destro; MS, medio sinistro; ID, inferiore destro; IS, inferiore sinistro

^aPercentuale di parenchima polmonare coinvolto da parte dell'intrappolamento d'aria per paziente

^bB, bronchiectasi; IPB, ispessimento della parete bronchiale; br, bronchiolettasi; ipb, ispessimento della parete bronchiolare

Discussion

WG is part of a diverse group of diseases characterised by a necrotising granulomatous vasculitis [1]. The disease affects about 3:100,000 people – men and women equally – and can occur at any age (mean 41 years) and, in comparison with other vasculitides, the lung is the most commonly affected organ, with a very aggressive airway pathology and chronic relapsing course [17, 18]. The lungs are affected in about 85% of patients. Traditionally, airway involvement in WG affects the trachea and the main bronchi as well as the segmental bronchi, mainly causing bronchial wall thickening and consecutive airway stenosis. Upper airway involvement occurs in 95% of cases. Subglottic tracheal and main bronchial stenosis occurs in about 20% of patients [17–20].

In contrast to the well-described pulmonary parenchymal involvement in WG, the lower airway disease manifestations are less well recognised by clinicians, and little is known from the literature [21–23]. In the study by Travis et al., open lung biopsy was performed in 67 patients with WG, and a variety of bronchial/bronchiolar lesions were noted, including acute and chronic bronchiolitis (51% and 64%, respectively), follicular bronchiolitis (28%) and bronchiolitis obliterans (31%). As stated in the study, these minor findings were often found in the periphery of typical nod-

ules of WG [22]. Similar findings were reported by Frazier et al. [24]. In other studies, small airway abnormalities in WG were characterised as unusual manifestations, including bronchiectasis and peribronchial thickening [25–28].

Interestingly, no patient in our study had tracheal or main bronchial involvement. Instead, 14 patients had airway involvement; in nine of them (42.8%), segmental and subsegmental bronchiectasis was recorded; in five (23.8%) bronchial wall thickening; in five (23.8%) bronchiolectasis; in two (9.5%) bronchiolar wall thickening (Figs. 4, 6). It is worth mentioning that all patients who presented with mild dyspnoea, dry cough, haemoptysis and inspiratory or expiratory wheezing had bronchial and bronchiolar involvement on inspiratory scans. Based on these results, HRCT appears to be capable of demonstrating segmental, subsegmental, bronchial and bronchiolar involvement in patients with WG, and the small airways may also be affected.

In normal individuals who are nonsmokers and have no history of exposure to organic or inorganic substances, the attenuation difference increases on expiratory HRCT by about 150 HU compared with inspiratory scans [15, 29]. According to the Fleischner's Society glossary for thoracic imaging, AT is retention of air in the lung distal to an obstruction [30]. It is well known that areas of AT show significantly less attenuation increase on expiration than in

normal lung, combined with a lack of volume reduction in these areas [30]. Usually, an attenuation increase of <80 HU between inspiration and expiration may be indicative of AT, so that comparison between inspiratory and expiratory CT scans may be helpful when AT is subtle or diffuse [30, 31].

Interestingly, AT areas were depicted in one-third of our patients (seven 33.3%) on expiratory chest HRCT scans. In six (28.5%) of these seven patients, AT was found to be multifocal. The most frequent AT distribution pattern was segmental (n=4, 19%), which together with the lobar pattern (n=1, 4.7%) are reported to be pathological and highly suggestive of small-airway disease [12, 13]. The probability of these AT areas being pathological is higher if we consider that none of these patients was a smoker or suffered from asthma or chronic obstructive pulmonary disease.

The finding of AT was bilateral in most patients (85.7%), whereas the distribution was in four lung fields (six fields in total) in both lungs in 5/7 patients (71.4%). This confirms the diffuse involvement of lung parenchyma due to vasculitis, which is a systemic inflammatory disease, and this explains the geographical distribution of AT areas.

In our study group, the attenuation difference of AT areas between expiratory HRCT and inspiratory scans ranged from 32 to 89 HU (mean 60.1 ± 23.5 HU). Generally, most patients with AT visible on expiratory HRCT also have abnormal findings on inspiratory scans [32]. In our study, 5/7 patients with AT areas on expiration had abnormal findings on inspiratory chest HRCT (Fig. 1). It is noteworthy that two of the 21 patients who were nonsmokers had no HRCT findings on inspiration and presented with AT areas on expiration (Fig. 1). As a consequence, in some cases, AT may present as the only abnormal HRCT finding indicating small-airway involvement in WG.

The three major pathological manifestations of classical WG observed in open lung biopsies are also useful di-

agnostic criteria, as stated by Travis et al. and include: (a) parenchymal necrosis, (b) vasculitis and (c) granulomatous inflammation accompanied by an inflammatory infiltrate composed of a mixture of neutrophils, lymphocytes, plasma cells, histiocytes and eosinophils [22]. Our hypothesis concerning the AT finding is that it may be related to endoluminal formation of granulomas as well as to abnormal thickening of the bronchial and bronchiolar walls, causing bronchiectasis and bronchiolectasis and consequently AT. This hypothesis clearly needs to be verified.

Finally, the mean values of the total extent of AT areas showed no statistically significant difference ($p > 0.005$) between the predominant patterns on inspiratory HRCT scans, such as pulmonary nodules, masses, ground-glass opacities, honeycombing and consolidation areas and the extent of airway involvement, including bronchial and bronchiolar wall thickening and the bronchiectasis and bronchiolectasis recorded in these patients.

Conclusions

HRCT in WG patients on deep inspiration may present various findings, such as nodules, ground-glass opacities, consolidation areas and honeycombing. Little is known about small-airway involvement in this rare disease. AT on deep expiratory HRCT scans could represent an additional, indirect finding that may indicate small airway involvement in about one third of patients. Especially in the absence of inspiratory findings, the presence of AT may unveil pulmonary involvement in WG, playing an important role in the therapeutic approach to these patients. As a consequence, we suggest that AT should be estimated on expiratory chest HRCT in every patient with WG and possible pulmonary involvement.

Conflict of interest None

References/Bibliografia

1. Reuter M, Schnabel A, Wesner F et al (1998) Pulmonary Wegener's granulomatosis: correlation between high-resolution CT findings and clinical scoring of disease activity. *Chest* 114:500–506
2. Cordier J-F, Valeyre D, Guillemin L et al (1990) Pulmonary Wegener's granulomatosis: a clinical and imaging study of 77 cases. *Chest* 97:906–912
3. Hoffman GS, Kerr GS, Leavitt RY et al (1992) Wegener granulomatosis: an analysis of 158 patients. *Ann Intern Med* 116:448–498
4. ATS/ERS (2002) International multidisciplinary consensus classification of idiopathic interstitial pneumonias. *Am J Respir Crit Care Med* 165:277–304
5. Komocsi A, Reuter M, Heller M et al (2003) Active disease and residual damage in treated Wegener's granulomatosis: an observational study using pulmonary high-resolution computed tomography. *Eur Radiol* 13:36–42
6. Leavitt RY, Fauci AS, Bloch DA et al (1990) The American College of Rheumatology criteria for the classification of Wegener's granulomatosis. *Arthritis Rheum* 33:1101–1107
7. Jennette CJ, Falk RJ, Andrassi K et al (1994) Nomenclature of systemic vasculitides: proposal of an international consensus conference. *Arthritis Rheum* 37:187–192

8. Weibel ER, Taylor CR (1988) Design and structure of the human lung. In: Fishman AP (ed) *Pulmonary diseases and disorders*. McGraw-Hill, New York, pp 11–60
9. Naidich DP, Webb WR, Grenier PA et al (2005) In: *Imaging of the airways: functional and radiologic correlations*. Lippincott Williams & Wilkins, Philadelphia
10. Fraser RS, Muller NL, Colman N, Pare PD (1999) Bronchiectasis and other bronchial abnormalities. In: Fraser RS, Muller NL, Colman N, Pare PD (eds) *Diagnosis of diseases of the chest*, 4th edn. W.B. Saunders Company, Philadelphia, pp 2265–2297
11. Austin JHM, Muller NL, Friedman PJ et al (1996) Glossary of terms for CT of the lungs: recommendations of the Nomenclature Committee of the Fleischner Society. *Radiology* 200:327–331
12. Mastora I, Remy-Jardin M, Sobaszek A et al (2001) Thin-section CT finding in 250 volunteers: assessment of the relationship of CT findings with smoking history and pulmonary function test results. *Radiology* 218:695–702
13. Tanaka N, Matsumoto T, Miura G et al (2003) Air trapping at CT: high prevalence in asymptomatic subjects with normal pulmonary function. *Radiology* 227:776–785
14. Webb WR, Muller LN, Naidich PD (2009) In: *High resolution CT of the lung*, 4th edn. Lippincott Williams & Wilkins/Wolters Kluwer
15. Webb WR, Stern EJ, Kanth N et al (1993) Dynamic pulmonary CT findings in normal adult men. *Radiology* 186:117–124
16. Stern EJ, Webb WR (1994) Dynamic quantitative computed tomography: a predictor of pulmonary function in obstructive lung diseases. *Invest Radiol* 29:564–569
17. Lohrmann C, Uhl M, Kotter E, Burger D et al (2005) Pulmonary manifestations of Wegener granulomatosis: CT findings in 57 patients and review of the literature. *Eur J Radiol* 53: 471–477
18. Langford AC (2005) Update on Wegener's granulomatosis. *Cleveland Clin J Med* 72: 689–697
19. Zycinska K, Wardyn KA, Zycinski Z, Zielonka TM (2008) Association between clinical activity and high-resolution tomography findings in pulmonary Wegener's granulomatosis. *J Physiol Pharmacol* 59:833–838
20. Gurney WJ, Winer-Muram TH, Stern JE et al (2006) *Diagnostic Imaging – Chest*, Amirsys Inc
21. Lee SK, Kim ST, Fujimoto K et al (2003) Thoracic manifestation of Wegener's granulomatosis: CT findings in 30 patients. *Eur Radiol* 13:43–51
22. Travis WD, Hoffman GS, Leavitt RY et al (1991) Surgical pathology of the lung in Wegener's granulomatosis. Review of 87 open lung biopsies from 67 patients. *Am J Surg Pathol* 15:315–333
23. Polychronopoulos VS, Prakash UB, Goblin JM et al (2007) Airway involvement in Wegener's granulomatosis. *Rheum Dis Clin North Am* 33:755–775
24. Frazier AA, Rosado-de-Christenson LM, Galvin RJ, Fleming VM (1998) Pulmonary angiitis and granulomatosis: radiologic-pathologic correlation. *Radiographics* 18:687–710
25. Maskell GF, Lockwood CM, Flower CDR (1993) Computed tomography of the lung in Wegener's granulomatosis. *Clin Radiol* 48:377–380
26. Papiris SA, Manoussakis MN, Drosos AA et al (1992) Imaging of thoracic Wegener's granulomatosis: the computed tomographic appearance. *Am J Med* 93:529–536
27. Weir IH, Muller NL, Chiles C et al (1992) Wegener's granulomatosis: findings from computed tomography of the chest in 10 patients. *J Can Assoc Radiol* 43:31–34
28. Foo SS, Weisbrod GL, Herman SJ, Chamberlain DW (1990) Wegener's granulomatosis presenting on CT with atypical bronchovascular distribution. *J Comput Assist Tomogr* 14:1004–1006
29. Stern EJ, Frank MS (1994) Small airway disease of the lungs: findings at expiratory CT. *AJR* 163:37–41
30. Hansell MD, Bankier AA, MacMahon H (2008) *Fleischner Society: Glossary of terms for thoracic imaging*. *Radiology* 246:697–722
31. Aquino SL, Webb WR, Golden J (1994) Bronchiolitis obliterans associated with rheumatoid arthritis: findings on HRCT and dynamic expiratory CT. *J Comput Assist Tomogr* 18:555–558
32. Arakawa H, Webb WR (1998) Air trapping on expiratory high-resolution CT scans in the absence of inspiratory scan abnormalities: correlation with pulmonary function tests and differential diagnosis. *AJR* 170:1349–1353